Some properties of the Irvine cable model and their use for the kinematic analysis of cable-driven parallel robots

J-P. Merlet

HEPHAISTOS project, Université Côte d'Azur, Inria, France

Abstract

Cable model has a strong influence on the complexity of the kinematic analysis of cable-driven parallel robots (CDPR). The most complete elasto-static model relies on Irvine equation that takes into account both the elasticity and the deformation of the cable due to its own mass and has been shown to be very realistic. This model is complex, non algebraic and numerically ill-conditioned, thereby leading to difficulties when using it in a kinematic analysis involving several cables. We exhibit some properties of this model that may drastically improve the analysis computation time when used in kinematic studies.

Keywords: cable-driven parallel robots, cable model, sagging cables

1. Introduction

Cables are essential elements in cable-driven parallel robots (CDPR) in which grounded winches independently pay off and reel in cables wound on a drum and attached to a moving platform at the other end. Such a robot has the advantages of parallel robots (accuracy, high velocity, large payload) but also may exhibit large workspace as illustrated by the FAST telescope robot [1], the COGIRO robot of Tecnalia/LIRMM [2] and our MARIONET-CRANE prototype [3] (figure 1).

Most of the works related to CDPR assume *ideal cables* without elasticity and deformation due to the cable mass. With that model the distance L_r between the attachment point B of the cable on the CDPR platform and the winch output point A is exactly the paid off cable length L_0 as measured. However the no-elasticity assumption does not hold for large CDPR with a difference between L_0, L_r of several centimeters or a variation evaluated at

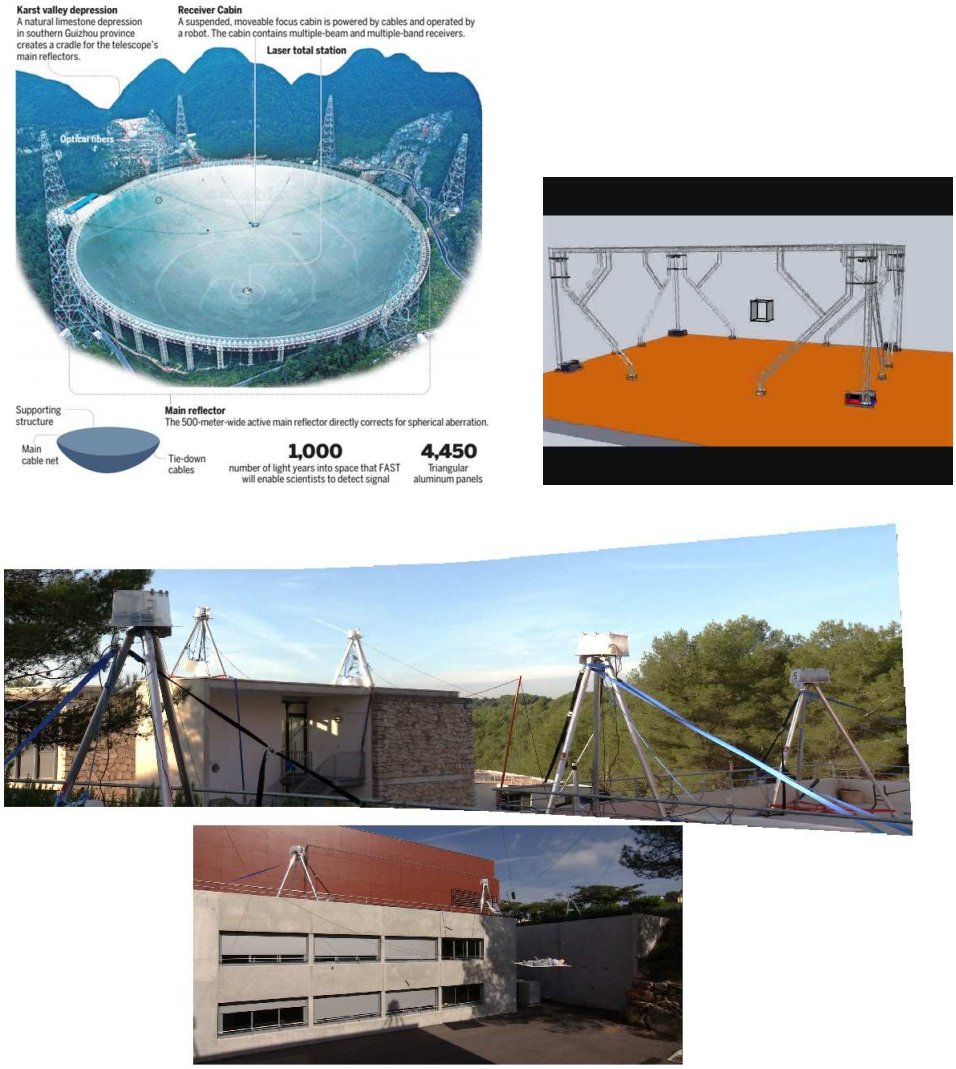

Figure 1: Large CDPR: the FAST telescope, the COGIRO robot and our MARIONET-CRANE prototype. The sagging effect on the later CDPR may easily be seen in the video part of the Hephaistos web site.

1% for a small CDPR [4]). As we will see the deformation of the cable due to its own mass induces also significant changes (see figure 3). Neglecting these effects will incur significant errors on the positioning of the CDPR but also on other state variables of the robot such as cable tensions or velocities.

In this paper we will consider the elasto-static Irvine sagging cable model that has been proposed for elastic and deformable cable with mass [5] and that has been shown to be in very good agreement with experimental results [6]. This model assumes that the cable lies in a vertical plane, the *cable plane*, and is therefore a 2D model. There are also other models that take into account torsion, out-of-plane motion [7, 8], the multi-strand nature of the cable [9] or specific to synthetic rope [9, 10, 11, 12, 13] but they are mostly valid for cables with a much larger diameter than the one used for CDPR or for cables having a very specific structure. Lumped-mass model have also been proposed [14] but we will see that they are difficult to use for CDPR.

A global reference frame $O, (x_r, y_r, z_r)$ is defined, with z corresponding to the upward local vertical, and a cable reference frame $A_i, (x, z = z_r)$ is defined in this plane with its origin at A_i, one of the extremity of the cable and x in the cable plane, being perpendicular to $z = z_r$. The coordinates of the other cable extremity B_i are $(x_b \geq 0, z_b)$ and we will assume that B_i is below A_i so that $z_b \leq 0$ (Assumption 1). Vertical and horizontal forces $F_z, F_x > 0$ are exerted by the platform on the cable at point B_i (figure 2).

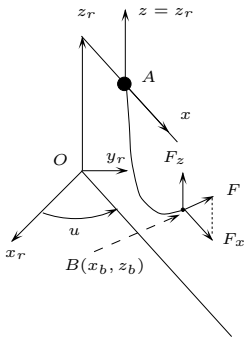

Figure 2: Notation for a sagging cable

Note that F_z is negative if the platform is exerting a downward force at B (the tangent of the cable at B has a negative z component), while F_z is positive of the tangent of the cable at B has a positive z component.

For a cable with length at rest L_0 the coordinates of B are given by the Irvine equations [5]:

$$x_b = F_x\left(\frac{L_0}{EA_0} + \frac{sinh^{-1}(\frac{F_z}{F_x}) - sinh^{-1}(\frac{F_z-\mu g L_0}{F_x})}{\mu g}\right) \quad (1)$$

$$z_b = \frac{F_z L_0 - \mu g L_0^2/2}{EA_0} + \frac{\sqrt{F_x^2+F_z^2} - \sqrt{F_x^2+(F_z-\mu g L_0)^2}}{\mu g} \quad (2)$$

where E is the Young modulus of the cable material, A_0 the cable cross-section area and μ the cable linear density. For example we may illustrate the influence of the cable deformation for a steel cable of diameter 6mm, length $L_0 = 50$ meters with infinite E (and therefore no elasticity) and $\mu = 0.346kg/m$ under a tension of 100 N by plotting the difference $L_0 - L_r$ as a function of F_x (figure 3). As may be seen in the figure there is a significant difference between L_0 and L_r and this change will directly affect the CDPR platform positioning.

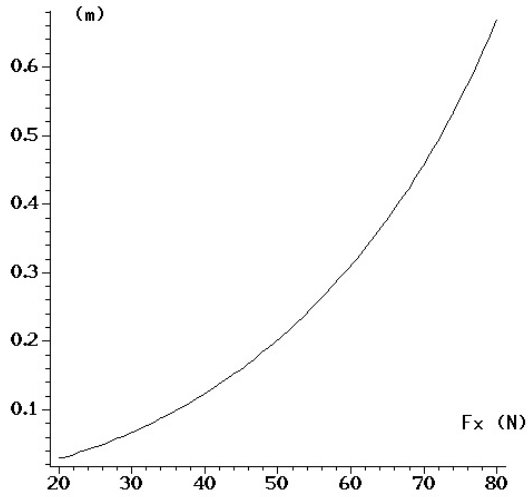

Figure 3: Difference in meter between the cable length and the distance between the attachment points A, B as function for F_x (N) for a total tension of 100N and a cable length at rest of 50 meters. This figure clearly shows that the sagging effect induces a large difference between the measured cable length and the distance between A, B as soon as F_x increases.

As may be seen on the figure the cable deformation induces a significant

difference between the distance between A, B and the cable length. Neglecting these effects will introduce error in the kinematic analysis of CDPR.

Another interesting property of the Irvine equations is that when $E \to \infty, \mu \to 0$, then they provide exactly the ideal cable model [15]. This point has been used in [15], [16] to propose algorithms for solving the inverse and direct kinematics of CDPR. The main idea of these algorithms is to start with the solutions of these problems for ideal cables (ie. $E = \infty, \mu = 0$) and for each of these solutions to incrementally move E, μ toward their real values, using a guaranteed Newton scheme to find the new solution at each step. Another interest of the Irvine equations is that they provide a very compact description of the cable effect with very few physical parameters, namely E, μ. The μ parameter may easily been estimated accurately, while E is more difficult to estimate and is time-varying. However we believe that an auto-calibration of E (which is outside the scope of this paper) based on additional sensors giving information on the state of the robot (see [17] for example) is doable. On the other hand using the lumped-mass model [14] will require much more parameters (number and location of the nodes, mass and spring stiffness) that are difficult to estimate and has never been proven experimentally for CDPR. Furthermore the low number of parameters in the Irvine equations allows one to manage uncertain values with interval analysis, while increasing the number of parameters will make this task much more difficult.

Equations (1,2) have as variables x_b, z_b, L_0, F_x, F_z. In the remaining sections of this paper we will consider that a combination of these variables have known values and we will determine closed-form solution for the remaining variables or univariate polynomials in one of the variable for which the maximal number of roots will be established. Some works have addressed this topic especially assuming that 3 of these 5 variables have a fixed value and establishing 2 equations for the remaining variables[18] whose solution is determined numerically. Our first contribution will be to establish new relationships between the variables that have not, to the best of the author knowledge, been proposed before.

Our second contribution addresses the use of these new relationships for the solving of the inverse and direct kinematics (IK and DK) of CDPR for which the cable model will obviously play an essential role. Cable model also influences the static analysis whose purpose is to determine the tension in the cables [19].

For the IK n cables are attached to a rigid body in a known pose (hence

the cable plane and the x_b, z_b of each cable are known) with the purpose of determining L_0. One may notice that (1,2) in their current form do not provide a closed-form for L_0. Hence solving the IK requires solving an equation system in $2n$ equations (1,2) with $3n$ unknowns and of the mechanical equilibrium of the platform that imposes 6 additional equations. If $n = 6$ we end-up with a square system of equations [20],[21],[22], To solve the IK authors have used optimization or have assumed that the solution is sufficiently close to the rigid leg case which is therefore used as initial guess for a solving based on the Newton scheme. However these methods cannot with certainty find all the solutions (as it has already be proven that the IK may have multiple solutions).

In the DK problem the n L_0 are known and the platform poses have to be determined. The unknowns are here the 6 parameters that define the platform pose and the $2nF_x, F_z$ while the constraints are the $2n$ equations (1,2) and the 6 equations of the mechanical equilibrium, so that we have always a square system that has usually multiple solutions. Note however that the DK assumes the measurement of L_0 while current systems provided the stressed length so that corrective steps should theoretically be applied. As equations(1,2) are not algebraic we cannot use methods such as elimination or Groebner basis that may provide all solutions for the DK and IK. Continuation method [23] are an option but requires a starting point. A natural starting point is to consider the cables as ideal and using the solutions of the IK and DK. However singularity are crossed during the continuation and are difficult to manage [16, 24]. It was recently proposed to solve the DK by looking at the minima of the potential energy of CDPR [25] but finding numerically all these minima is tedious and uncertain.

We have addressed the IK and DK solving issues in previous publications, using as solving method an interval analysis-based approach that is guaranteed to provide all solutions assuming that the unknowns are bounded [26, 27] and is able to manage different cable models. The next section presents the principle of solving based on interval analysis and explains how the additional relationships we will provide in this paper may speed-up the solving. Note that this paper is an extended version of the conference paper [28] with new results and examples that illustrate the use of this work for the kinematic analysis of CDPR.

2. Interval analysis

Interval analysis is based on *interval evaluation* of a function f in the unknowns $\{x_1, x_2, \ldots x_n\}$ that are supposed to be bounded i.e. for each x_i we have $x_i \in [\underline{x_i}, \overline{x_i}]$ where $\underline{x_i}, \overline{x_i}$ are respectively the lower and upper bound for x_i. Such bounds define a *box* in the n-dimensional space of the unknowns. Being given such a box $\mathcal{B}$ the interval evaluation $\hat{f}$ of f over $\mathcal{B}$ is an interval $[\underline{f}, \overline{f}]$ such that for any point X in $\mathcal{B}$ we have $\underline{f} \leq f(X) \leq \overline{f}$. In other words $\underline{f}$ is either equal to or a minorant of the minimum f_{min} of f over $\mathcal{B}$ while $\overline{f}$ is equal to or a majorant of the maximum f_{max} of f over $\mathcal{B}$. The interval evaluation of f is relatively easy to obtain if f is expressed in terms of classical mathematical functions using the *natural evaluation* which basically consist in replacing the operators by interval equivalents. For example interval evaluation of the Irvine equations may be obtained by natural evaluation. A property of interval analysis is that two mathematically equivalent forms of f may have different interval evaluations. For example $f^1 = x^2 + 2x + 1$ and $f^2 = (x+1)^2$ are equivalent but $\hat{f}^2$ will be tight with only one occurrence of x while $\hat{f}^1$ will not if $\underline{x} < 0$. A solving algorithm may then be designed just by discarding boxes for which we have for any equation in the set either $\underline{f} > 0$ or $\overline{f} < 0$ as this shows that there is no solution of this equation for the variable in the box. Otherwise the box is bisected: one variable is chosen and its range is bisected at its mid -point so that two new boxes are created differing just by this variable range. It is not needed to bisect a box until it is reduced to a point as sophisticated methods [29, 30, 31, 32] allow to determine if a single root is present in a box (provided that it is small enough) and provide a numerical method to calculate this root.

However the efficiency of interval algorithms is drastically dependent upon the *tightness* of the interval evaluation: the closer $\underline{f}, \overline{f}$ are to f_{min}, f_{max}, the faster will be the algorithm. An interval evaluation will be denoted *tight* if $\hat{f} = [f_{min}, f_{max}]$. But the natural evaluation may lead to large under or overestimation of the minimum and maximum as soon as there are multiple occurrences of the unknowns in f (it may be proven that if there is only a single occurrence of each unknown in f, then $\hat{f}$ is tight, up to round-off errors). The tightness will improve when the widths of the intervals for the unknowns decrease but an efficient way to improve the tightness of the evaluation is to consider the derivatives of f and their own interval evaluation. Let f_i be the derivative of f with respect to x_i and let $[\underline{f_i}, \overline{f_i}]$ be its interval

evaluation over $\mathcal{B}$. If $\underline{f_i} > 0$ or $\overline{f_i} < 0$, then f is monotonic with respect to x_i. Consequently $\hat{f}$ may be obtained as $[\mathrm{Min}\hat{f}(\mathcal{B}_i), \mathrm{Max}\hat{f}(\mathcal{B}_i)]$ where $\mathcal{B}_i$ are the boxes that are derived from $\mathcal{B}$ with x_i set to $\underline{x_i}$ or $\overline{x_i}$. Note that this process has to be applied recursively. Indeed assume that there is a $j > 1$ such that f is monotonic with respect to x_j (implying that $\hat{f}$ will be obtained using $\mathcal{B}_j$), while for $i < j$ this was not the case. But for $i < j$ the monoticity has been evaluated using $\mathcal{B}$ and as we are now using the tighter $\mathcal{B}_j$ the monoticity test may give another result. Using this process we may tighten the interval evaluation of f up to the point where $\hat{f} = [f_{min}, f_{max}]$ if f is such that all $f_i, i \in [1, n]$ are positive or negative. Besides the use of derivatives another method is usually efficient to decrease the computation time. Let us assume that an equation may be rewritten as $H(x_i) = G(x_1, \ldots x_{i-1}, x_{i+1} \ldots x_n)$ where H is an invertible function of x_i. Let $\hat{G} = [\underline{G}, \overline{G}]$ be the interval evaluation of G for a given box. The range $\hat{x_i}$ for the unknown x_i is updated by $\hat{x_i} \cap H^{-1}(\hat{G})$ and the box is discarded if this intersection is empty. We may also sharpen the range for x_i by computing $[\underline{x_i}, \underline{x_i} + \epsilon] \cap \hat{G}$ where ϵ is a small value: if this intersection is empty then the lower bound for x_i becomes $\underline{x_i} + \epsilon$ and we may repeat the process. A similar procedure may be used for the upper bound.

One difficulty of interval analysis is determining the right combination of heuristics that leads to the best computation time being given that this heuristics may reduce the computation time of the basic interval analysis algorithm from an almost intractable value to a few seconds.

Our second contribution is to present in the next sections some interesting properties of the Irvine equations that can be used for analysis or solving purposes.

3. Properties of the Irvine equations

A preliminary property will play an important role: we have assumed that B has an altitude that is equal or lower to the one of A with the direct consequence that $F_z \leq \mu g L_0/2$ (F_z must be lower than this value as soon as B is lower than A).

3.1. Derivatives of the Irvine equations

The sign of the derivatives of the Irvine equations may be obtained with interval evaluation but it is interesting to determine beforehand if they may be inherently monotonic.

Under assumption 1 we may establish the sign of derivatives of equations (1),(2) that will be presented without proof as they are trivial. We have

$$\frac{\partial z_b}{\partial L_0} < 0 \quad \frac{\partial z_b}{\partial F_z} > 0 \quad \frac{\partial z_b}{\partial F_x} > 0 \tag{3}$$

As all derivatives of z_b have a constant sign, then its interval evaluation for interval values for F_x, F_z, L_0 will always be tight and can be computed efficiently using only floating point operators. This may have an impact on the IK solving in which z_b has a fixed value: If $\hat{z_b} \cap z_b = \emptyset$, then (2) has no solution for the current F_x, F_z, L_0 box. We have also:

$$\frac{\partial x_b}{\partial L_0} > 0 \quad \frac{\partial x_b}{\partial F_z} > 0 \quad \frac{\partial x_b}{\partial F_x} > 0 \tag{4}$$

It may also be interesting to consider the distance $D = x_b^2 + z_b^2$ between A and B. We have $\partial D/\partial L_0 > 0$ but no general monotonicity can be obtained with respect to F_x, F_z.

Let F_x, F_z, L_0 being bounded i.e. $F_x \in [\underline{F_x}, \overline{F_x}]$, $F_z \in [\underline{F_z}, \overline{F_z}]$, $L_0 \in [\underline{L_0}, \overline{L_0}]$. Let us assume that z_b is fixed and consider the equation $f(L_0, F_z, F_x) - z_b = 0$. Using the implicit value theorem it may be shown that the solution of this equation satisfies

$$\frac{\partial F_x}{\partial L_0} > 0 \quad \frac{\partial F_x}{\partial F_z} < 0$$

so that F_x is restricted to lie in the interval $[\underline{F'_x}, \overline{F'_x}]$ where $\underline{F'_x}$ is the solution of (2) obtained for $L_0 = \overline{L_0}$, $F_z = \underline{F_z}$ and $\overline{F'_x}$ is the solution of (2) obtained for $L_0 = \underline{L_0}$, $F_z = \overline{F_z}$. The range for F_x may therefore be calculated as $[\underline{F_x}, \overline{F_x}] \cap [\underline{F'_x}, \overline{F'_x}]$ and the equation has no solution if this intersection is empty. More generally if we consider (2) when 2 of the unknowns are fixed and denotes its solution by S in the last unknown we get $[\underline{L'_0}, \overline{L'_0}] = [S(\overline{F_x}, \overline{F_z}), S(\underline{F_x}, \underline{F_z})]$ and $[\underline{F'_z}, \overline{F'_z}] = [(S(\underline{F_x}, \overline{L_0}), S(\overline{F_x}, \underline{L_0})]$.

3.2. New forms for the Irvine equation

We present in this section various new relationships between the quantities appearing in the Irvine equations. They are usually expressed in a semi-explicit form $H(X) = G(Y)$ where X is an element of the set $\{x_b, z_b, F_x, F_z, L_0\}$ while Y is the complementary of X with respect to this set. The function H will be invertible and its definition may impose some constraint on G. In the numerical examples we will set $E = 1^{11} N/m^2$, $\mu = 0.346 kg/m$ and the cable diameter to 6 mm.

3.2.1. Using the z_b equation

F_x as function of z_b, F_z, L_0.

Let

$$a^2 = F_x^2 + F_z^2 \qquad b^2 = F_x^2 + (F_z - \mu g L_0)^2 \quad a^2 - b^2 = \mu g L_0(2F_z - \mu g L_0) < 0$$

then z_b may be written as

$$z_b = (\frac{(a-b)}{\mu g})(\frac{(a+b)}{2EA_0} + 1) = \frac{L_0(2F_z - \mu g L_0)}{2EA_0} + \frac{a-b}{\mu g} \tag{5}$$

Let us assume now that z_b, F_z, L_0 are given so that (2) has only F_x as unknown. Our objective is to get an expression of this unknown. Let us define

$$a^2 = F_x^2 + F_z^2 \qquad b^2 = F_x^2 + (F_z - \mu g L_0)^2 \qquad U = \frac{L_0(F_z - \mu g L_0/2)}{EA_0} - z_b$$

so that equation (2) may be written as

$$U + \frac{(a-b)}{\mu g} = 0 \tag{6}$$

We have also

$$a^2 - b^2 = 2F_z \mu g L_0 - (\mu g L_0)^2 = V = (a+b)(a-b) = (a+b)(-U\mu g)$$

from which we get

$$b = -\frac{V}{U\mu g} - a$$

Reporting b in (6) leads to

$$2a = -U\mu g - \frac{V}{U\mu g} = W \tag{7}$$

Note that U, V are not function of F_x so that W is expressed only as a function of F_z, L_0. As $a^2 = (W/2)^2 = F_x^2 + F_z^2$ we get

$$F_x^2 = (W/2)^2 - F_z^2 \tag{8}$$

where the right-hand term is a function of F_z, L_0 only. This equation provides F_x if z_b, L_0, F_z are fixed but also imposes a constraint on $(W/2)^2 - F_z^2$ that should be positive.

Let's assume that F_z has an interval value and consider $P = F_x^2 = (W/2)^2 - F_z^2$ that is positive. The polynomial P is of degree 4 in F_z and factors out in 4 terms that are linear in F_z. The roots of P are

$$s_1 = \frac{\mu g L_0}{2} + \frac{\mu g A_0 E z_b}{2A_0E + \mu g L_0} \quad s_2 = \frac{\mu g L_0}{2} + (z_b - L_0)\frac{A_0 E}{L_0}$$

and

$$s_3 = \frac{\mu g L_0}{2} + (z_b + L_0)\frac{A_0 E}{L_0} \quad s_4 = \frac{\mu g L_0}{2} - \frac{\mu g A_0 E z_b}{2A_0E - \mu g L_0}$$

If we assume $2A_0E > \mu g L_0$ then the roots in F_z are ordered as $s_2, s_1(< \mu g L_0/2), s_4(> \mu g L_0/2), s_3$ and P will be positive if $F_z \in [s_2, s_1]$. If $2A_0E < \mu g L_0$ then the roots are ordered as $s_2, s_4(< \mu g L_0/2), s_1(< \mu g L_0/2), s_3$. Therefore there are 2 possible ranges for F_z leading to a positive P: $[s_2, s_4]$, $[s_1, \mu g L_0/2]$. The previously determined range for F_z may be used to update the range of several variables in an interval analysis based algorithm.

Numerical example: Consider the case where $L_0 \in [50, 50.4]$, $F_x \in [100, 130]$, $F_z \in [-130, -100]$. The interval estimation of z_b based on equation (2) is [-54.954,-30.586]. Using equation (8) leads to the range [0,286.34] for F_x. But if we restrict z_b to the range [-54.954,-49] or [-37,-30.586] the range for F_x as deduced from (8) does not have an intersection with the range [100,130]. Therefore we can claim that z_b is restricted to]-49,-37]: this interval is 7 times smaller than the one that has initially been obtained.

$\underline{L_0}$ **as function of** $\underline{z_b, F_z, F_x}$.
We are now interested in determining L_0 when F_x, F_z, z_b are fixed. Let $U_1 = \sqrt{F_x^2 + F_z^2}$, $U_2 = \mu g F_z/EA_0$, $U_3 = (\mu g)^2/(2EA_0)$ and $U_4 = -\mu g z_b + U_1$. Equation (2) may be written as

$$U_2 L_0 - U_3 L_0^2 + U_4 = \sqrt{F_x^2 + (F_z - \mu g L_0)^2} \tag{9}$$

Squaring the previous equation leads to

$$P_s = (U_2 L_0 - U_3 L_0^2 + U_4)^2 - (F_x^2 + (F_z - \mu g L_0)^2) = 0 \tag{10}$$

As U_1, U_2, U_3, U_4 are not functions of $L_0 > 0$ this equation is a fourth order polynomial in L_0. Using the Sturm sequences it is possible to show that P_s has only 2 roots for L_0 in the range $[0, \infty]$. One of these root leads to

$$U_2 L_0 - U_3 L_0^2 + U_4 = -\sqrt{F_x^2 + (F_z - \mu g L_0)^2}$$

that is not compatible with equation (9). Therefore solving P_s (whose roots may be obtained in analytical form but cannot be displayed here for lack of space) leads to a single solution for L_0. Note that for an interval-based algorithm we will first compute an interval evaluation of P_s to determine if it may have a zero and it is not necessary to use the analytical form of the roots to obtain bounds for L_0 using only the interval evaluation of the polynomial coefficients [33, 34]. As we may have a tight range for L_0 (e.g. in the DK problem) another possibility is to look at the Sturm sequences (or at the simpler Budan-Fourier sequence) of the polynomial for this range. whose elements are functions of F_x, F_z. If there is no root to the polynomial (10), then the number of sign changes for $\overline{L_0}$ minus the number of sign changes for $\underline{L_0}$ should be equal to 0, thereby inducing inequality constraints on F_x, F_z that may possibly allow one to tighten the ranges for these variables.

Numerical example: we assume that L_0 is measured and lie in the range [50,50.03] meter . A sensor on the platform allows to get an estimation of z_b as -42.3922 $\pm$ 0.05 meter. The force F_x is estimated to be in the range [100,110] while F_z is in the range [-130,-110]. An analysis of the Budan-Fourier sequence for $L_0 = 50$ and $L_0 = 50.03$ shows that the polynomial P_s has a root in the L_0 range only if $P_s(50) \times P_s(50.03) < 0$. An analysis of the derivatives of P_s with respect to F_x, F_z shows that they are positive. As for $F_x = 110$, $F_z = -110$ we have $P_s([50, 50.03]) < 0$ we deduce that the polynomial P_s has no root whatever the values of F_x, F_z in their respective range are.

$\underline{F_z}$ **as function of** $z_b, F_x, \underline{L_0}$.
We consider determining F_z for given L_0, F_x, z_b. Equation (8) is a 4th order polynomial Q in F_z with the constraint that $W > 0$. Using Budan-Fourier theorem [33] it is possible to show that Q has 0 or 2 roots in the range $]-\infty, \mu g L_0/2]$ but only one these roots will lead to a positive $W > 0$. The analysis of the sign of W is complex but it may be shown that if $EA_0 \gg \mu g L_0$, then F_z must belong to the range $[\mu g L_0/2 + EA_0 z_b/L_0, \mu g L_0/2 - \mu g z_b^2/(2L_0)]$.

3.2.2. Using the x_b equation

$\underline{F_z}$ **as function of** $x_b, F_x, \underline{L_0}$.
We consider the calculation of F_z being given F_x, L_0, x_b. We define

$$u = \frac{F_z}{F_x} \quad v = \frac{F_z - \mu g L_0}{F_x}$$

so that equation (1) may be written as

$$(\frac{x_b}{F_x} - \frac{L_0}{EA_0})\mu g = sinh^{-1}(u) - sinh^{-1}(v) \tag{11}$$

We define $H_1 = x_b/F_x - L_0/(EA_0)$ and we use the identity

$$sinh^{-1}(u) - sinh^{-1}(v) = sinh^{-1}(u\sqrt{1+v^2} - v\sqrt{1+u^2})$$

Using the the hyperbolic sine of both terms of equation (11) we obtain:

$$H(x_b, L_0, F_x) = sinh(H_1\mu g) = u\sqrt{1+v^2} - v\sqrt{1+u^2} \tag{12}$$

We have already defined $a^2 = F_x^2 + F_z^2$, $b^2 = F_x^2 + (F_z - \mu g L_0)^2$ so that $a^2 = F_x^2(1+u^2)$ and $b^2 = F_x^2(1+v^2)$. Equation (12) may therefore be written as:

$$F_x H(x_b, L_0, F_x) = ub - va \tag{13}$$

Note that the left-hand term of this equation is not a function of F_z. Let us define $W = F_x H(x_b, L_0, F_x)$ and u_1, u_2 such that $1 + u^2 = u_1^2$, $1 + v^2 = u_2^2$ so that

$$W = ub - va = F_z u_2 - u_1(F_z - \mu g L_0) \tag{14}$$

We have also $u_1^2 - u_2^2 = u^2 - v^2$ so that

$$u_1^2 - u_2^2 = (2F_z\mu g L_0 - (\mu g L_0)^2)/F_x^2 \tag{15}$$

Solving (14) for u_2 and reporting it in (15) leads to an equation in u_1, F_x, F_z, L_0, W which is of second order in u_1. Substituting $u_1^2 = (F_x^2 + F_z^2)/F_x^2$ in this equation lead to a linear equation in u_1. This equation is solved in u_1 and the result is reported in $u_1^2 = (F_x^2 + F_z^2)/F_x^2$ that becomes a polynomial of order 4 in F_z whose coefficients are functions of F_x, L_0, x_b

L_0 as function of x_b, F_x, F_z.

Consider equation $x_b - x_b^s$ where x_b^s is a desired value for x_b and x_b is provided by equation (1) and F_x, F_z are given. This equation may be written as

$$F(L_0) = u2L_0 - u_3 sinh^{-1}(u_4 + u_5 L_0) - u_1 = 0 \tag{16}$$

with $-u_1 = x_b^s/F_x - sinh^{-1}(F_z/F_x)/(\mu g)$, $u_2 = 1/(EA_0) > 0$, $u_3 = 1/(\mu g) > 0$, $u_4 = F_z/Fx$, $u_5 - -\mu g/F_x < 0$. Although it seems difficult to derive

a closed-form for the root in L_0 of this equation, it appears that F has interesting properties. Indeed the derivative of F with respect to L_0 is strictly positive, while $F(0) = -x_b^s/F_x < 0$, and consequently there is a single root in L_0 for $F = 0$. Furthermore as the term $u_2 L_0$ is positive if $-u_3 sinh^{-1}(u_4 + u_5 L_0) > u_1$, then $F > 0$. Further manipulation of this inequality leads to $F > 0$ if $L_0 > |u_5| sinh^{-1}(u_1/u_3)/u_4 = L_0^M$. Hence L_0^M is an upper bound for the root of $F = 0$. A simple dichotomy procedure allows one to obtain quickly an estimation of the root. At each step of the dichotomy we check if the Kantorovitch theorem conditions [35] hold for the current estimation of the root so that the Newton scheme will converge to the solution. Such a procedure leads to a very fast determination of the root, that may be obtained with an arbitrary accuracy. If F_x, F_z are provided as intervals, then rewriting F as $L_0 = (u_3 sinh^{-1}(u_4 + u_5 L_0) + u_1)/u_2$ may be useful to decrease the range for L_0.

Numerical example: we set $F_x = 1, F_z = -10, x_b^s = 0.5$. We obtain $L_0^M = 18.571$. For $L_0^m/2$ we get $F < 0$ so that we set $L_0 = (L_0^M/2 + L_0^M)/2 = 13.92855$. For that value the Kantorovitch conditions hold and the Newton scheme provide the solution $L_0 = 13.1732$.

F_x as function of x_b, L_0, F_z.

Consider equation $x_b - x_b^s$ where x_b^s is a desired value for x_b and x_b is provided by equation (1) and L_0, F_z are given. It seems difficult to derive a closed-form for the root in F_x of this equation. But we have shown in section 3.1 that $\partial x_b/\partial F_x$ is positive. As the limit of x_b when F_x goes to 0 is 0 while its limits when $F_x \to \infty$ is L_0. Hence this equation has a single root in F_x.

We note also that $x_b = F_x L_0/(EA_0) + \alpha$ where α is positive. Consequently we have $F_x L_0/(EA_0) < x_b$ or $F_x < EA_0 x_b/L_0$, this inequality providing an upper bound for the root of F_x. Hence a dichotomy process, mixed with the use of the Newton method as described in the previous section, will provide efficiently the root.

3.2.3. Using the x_b and z_b equations

F_z as function of x_b, z_b, F_x, L_0.

We proceed along the same direction than the calculation of F_z described in section 3.2.2 using the equation

$$F_x H(x_b, L_0, F_x) = ub - va \tag{17}$$

We have already established in section 3.2.1 the values of a, b as functions of z_b, L_0, F_z while u, v are functions of F_x, L_0, F_z. Hence the right-hand term of (17) is a function of z_b, L_0, F_x, F_z. This function is a third order polynomial P_3 in F_z. Using the Sturm sequence [33] and the constraint $a > 0$ it is possible to show that P_3 has a single real root in the range $]-\infty, \mu g L_0/2]$.

Numerical example: we assume $x_b \in [24.65, 24.8]$, $z_b \in [-43.5, -43]$, $F_x \in [90, 100]$, $F_z \in [-90, -85]$ and $L_0 \in [49, 49.02]$. The number of sign changes of the Budan-Fourier sequence for $F_z = -90$ and for $F_z = -85$ are both one so that P_3 has no root in its interval.

zb **as a function of** x_b, F_x, F_z, L_0.
Equation (2) provides a mean of calculating z_b when F_x, F_z, L_0 are known but does not involve x_b and we provide here another form that involves x_b. Using the notation and result of section 3.2.3 we get:

$$z_b = \frac{L_0}{F_z}(\sqrt{F_x^2 + F_z^2} - \frac{F_x^2}{\mu g L_0} sinh(\mu g(\frac{x_b}{F_x} - \frac{L_0}{EA_0}))) + \frac{L_0(F_x - \mu g L_0/2)}{EA_0} \tag{18}$$

Note that we may also obtain a bound on the cable tension $\sqrt{F_x^2 + F_z^2}$ at B as

$$\sqrt{F_x^2 + F_z^2} = \frac{F_x^2}{\mu g L_0} sinh(\mu g(\frac{x_b}{F_x} - \frac{L_0}{EA_0})) + F_z(\frac{z_b}{L_0} + \frac{\mu g L_0}{2EA_0} - \frac{F_z}{EA_0}) \tag{19}$$

3.3. Using the cable tangents

Sensors may provide a relatively accurate measurement of the cable tangents $v = (F_z - \mu g L_0)/F_x$ at A and $u = F_z/F_x$ at B [17]. Under the assumption that u, v are known we get

$$F_x = \frac{\mu g L_0}{(u - v)} \qquad F_z = uF_x \qquad F_x^2 + F_z^2 = (\frac{\mu g L_0}{(u - v)})^2(1 + u^2) \tag{20}$$

A trivial transformation of (2) leads to:

$$\mu\, g {L_0}^2(u + v) + 2\, A_0\, E L_0(\sqrt{u^2 + 1} - \sqrt{v^2 + 1}) + 2\, z_b\, E A_0(v - u) = 0 \tag{21}$$

which is a quadratic polynomial in L_0 whose coefficients are functions of u, v, z_b. It is easy to show that this polynomial has a single positive root. Now equation (1) may be written as

$$F_x(\frac{L_0}{EA_0} + \frac{(sinh^{-1}(u) - sinh^{-1}(v))}{\mu g}) - x_b = 0 \tag{22}$$

As we have $F_x = \mu g L_0/(u-v)$ this equation may be transformed in a second order polynomial in L_0 whose coefficients are functions of u, v, x_b. Here again it is easy to show that this polynomial has at most one positive root.

As $F_z = uF_x$ and $L_0 = (F_x(u-v))/(\mu g)$ equations (11), (22) are polynomials in F_x with coefficients that are functions of u, v. The resultant of these equations in F_x establishes a polynomial relationship between x_b, z_b which is a quadric, more precisely a *parabola* which is written as

$$(Ax_b + Cz_b)^2 + Dx_b + Fz_b = 0 \tag{23}$$

with

$$A = \sqrt{\mu g}(u-v)(u+v) \qquad C = -2\sqrt{\mu g}(u-v)$$
$$D = 2EA_0(u-v)(R_1\mu g(u+v) - 2R_2)R_2$$
$$F = -2\mu g EA_0(u-v)(R_1\mu g(u+v) - 2R_2)R_1$$
$$R_1 = (sinh^{-1}(u) - sinh^{-1}(v))/(\mu g) \qquad R_2 = \sqrt{1+u^2} - \sqrt{1+v^2}$$

Note that if $EA_0 \gg \mu g L_0$, then A, C are small and D, F very large so that the parabola is very close to a line.

The measurements of $u, v.L_0$ provide a direct estimation of $F_x = \mu g L_0/(u-v)$ and consequently of $F_z = uF_x$ and therefore of the cable tension at B without any force sensor. As these measurements are uncertain (however with a bounded uncertainty) we will get a range for x_b, z_b using equations (1,2) that may possibly be sharpened using the parabola equation (23). These sharpened evaluations may possibly be used to sharpen either L_0, u, v and/or F_x, F_z.

3.4. Summary

Each of the two Irvine equations involves 4 variables: x_b (or z_b), F_x, F_z, L_0. Consequently each equation may be used to determine one of the variables if the other 3 variables are known. If both equations are used we have 5 variables. If 3 of them are known the Irvine equations become a system of 2

equations in 2 unknowns and we may, theoretically, obtain these 2 unknowns as functions of the known variables. We have not been able to reach this goal (except for the trivial case where x_b, z_b are the unknowns). However if we assume that 4 variables are known, then the Irvine equations are over-constrained and may be used to calculate the remaining unknown. Table 1 summarizes the obtained result. In this table the unknown are presented as F_x, F_z, L_0, x_b, z_b. For one unknown there are several columns. Each of this column is either empty or has a $\bullet$ or a $\div$ symbol. A column with only $\bullet$ indicates that the unknown can be calculated in closed-form if the indicated variables are set. A column with only $\div$ indicates that the unknown has not been obtained in closed-form but that an efficient numerical scheme can be designed to calculate the unknown. For example the first column for the unknown F_x shows that F_x can be calculated in closed-form if F_z, L_0, z_b are known, while the second column shows that F_x can be calculated numerically if F_z, L_0, x_b are known.

	F_x		F_z			L_0		x_b	z_b	
F_x	-		$\bullet$	$\bullet$	$\bullet$	$\bullet$	$\div$	$\bullet$	$\bullet$	$\bullet$
F_z	$\bullet$	$\div$	-			$\bullet$	$\div$	$\bullet$	$\bullet$	$\bullet$
L_0	$\bullet$	$\div$	$\bullet$	$\bullet$	$\bullet$	-		$\bullet$	$\bullet$	$\bullet$
x_b		$\div$		$\bullet$	$\bullet$		$\div$	-		$\bullet$
z_b	$\bullet$		$\bullet$		$\bullet$	$\bullet$			-	

Table 1: Summary of the result showing how the unknown indicated in the first row can be be obtained as function of the variables indicated in the first vertical column.

4. Conclusion

We have presented in this paper various results regarding the Irvine equations that may be useful both for analysis and solving of kinematic equations that rely on this cable model as they establish a more general view of the underlying structure of this model. We have shown that the proposed new forms of the Irvine equations may be useful to speed up the solving of the IK and DK of CDPR based on interval analysis (part of them have been implemented our CDPR IK and DK solver with a strong influence on the solving time for finding all solutions). But they may possibly also be used for alternate solving methods such as continuation. It must be reminded that

all these solving methods are not intended to be used for real-time computation (i.e. within the sampling time of the CDPR controller) as generic and guaranteed Newton scheme exists for that purpose. Still open issues on the CDPR with sagging cables such as workspace and singularity analysis may benefit from this new approach to the Irvine equations.

Acknowledgement:
This paper has been partly supported by Agence Nationale de la Recherche (ANR), under grant ANR-18-CE10-0004-03 (CRAFT project)

References

[1] X. Tang, R. Yao, Dimensional design of the six-cable driven parallel manipulator of FAST, ASME J. of Mechanical Design 133 (11) (November 2011) 111012–1/11.

[2] M. Gouttefarde, D. Nguyen, C. Baradat, Kinetostatics analysis of cable-driven parallel robots with consideration of sagging and pulleys, in: ARK, Ljulbjana, June 29- July 3, 2014, pp. 213–221.

[3] J.-P. Merlet, D. Daney, A portable, modular parallel wire crane for rescue operations, in: IEEE Int. Conf. on Robotics and Automation, Anchorage, May, 3-8, 2010, pp. 2834–2839.

[4] V. Schmidt, A. Pott, Investigating the effect of cable force on winch winding accuracy for cable-driven parallel robots, Proceedings of the Institution of Mechanical Engineers, Part K: Journal of Multi-body Dynamics 230 (3) (2016) 237–241.

[5] H. M. Irvine, Cable Structures, MIT Press, 1981.

[6] N. Riehl, et al., On the determination of cable characteristics for large dimension cable-driven parallel mechanisms, in: IEEE Int. Conf. on Robotics and Automation, Anchorage, May, 3-8, 2010, pp. 4709–4714.

[7] M. Ahmadi-Kashani, A. Bell, The analysis of cables subject to uniformly distributed loads, Eng. Struct. 10 (1988) 174–182.

[8] H. Hussein, M. Gouttefarde, F. Pierrot, Static modeling of sagging cables with flexural rigidity and shear forces, in: ARK, Bologna, July, 1-5, 2018.

[9] S. Ghoreishi, et al., Analytical modeling of synthetic fiber rope. part II: a linear elastic model for 1+6 fibrous structure, Int. J. of Solids and Structures (2007) 2943–2966.

[10] J. Piao, et al., Open-loop position control of a polymer cabledriven parallel robot via a viscoelastic cable model for high payload workspaces, Advances in Mechanical Engineering 9 (12).

[11] W. Samuel, et al., Synthetic mooring rope for marine renewable energy applications, Renewable energy 83 (November 2015) 1268–1278.

[12] V. Schmidt, Modeling techniques and reliable real-time implementation of kinematics for cable-driven parallel robots using polymer fiber cables, Ph.D. thesis, Université Stuttgart (June, 20, 2016).

[13] P. Tempel, F. Trautweing, A. Pott, Experimental identification of stress-strain material models of UHMWPE fiber cables for improving cable tension control strategies, in: ARK, Bologna, July, 1-5, 2018.

[14] J. Kamman, R. Huston, Multibody dynamics modeling of variable length cable systems, Multibody System Dynamics 5 (3) (2001) 211–221.

[15] J.-P. Merlet, A new generic approach for the inverse kinematics of cable-driven parallel robot with 6 deformable cables, in: ARK, Grasse, June, 27-30, 2016.

[16] J.-P. Merlet, Preliminaries of a new approach for the direct kinematics of suspended cable-driven parallel robot with deformable cables, in: Eucomes, Nantes, September, 20-23, 2016.

[17] J.-P. Merlet, An experimental investigation of extra measurements for solving the direct kinematics of cable-driven parallel robots, in: IEEE Int. Conf. on Robotics and Automation, Brisbane, 2018.

[18] D. Papini, On shape control of cables under vertical static loads, Master's thesis, Lund University, Lund (2010).

[19] L. Hui, A giant sagging-cable-driven parallel robot of FAST telescope: its tension-feasible workspace of orientation and orientation planning, in: 14th IFToMM World Congress on the Theory of Machines and Mechanisms, Taipei, October, 27-30, 2015.

[20] K. Kozak, et al., Static analysis of cable-driven manipulators with non-negligible cable mass, IEEE Trans. on Robotics 22 (3) (June 2006) 425–433.

[21] N. Riehl, et al., Effects of non-negligible cable mass on the static behavior of large workspace cable-driven parallel mechanisms, in: IEEE Int. Conf. on Robotics and Automation, Kobe, May, 14-16, 2009, pp. 2193–2198.

[22] D. Sridhar, R. Williams II, Kinematics and statics including cable sag for large cable suspended robots, Global Journal of Researches in Engineering: H Robotics & Nano-Tec 17 (1).

[23] E. Allgower, Numerical continuation methods, Springer-Verlag, 1990.

[24] J.-P. Merlet, A generic numerical continuation scheme for solving the direct kinematics of cable-driven parallel robot with deformable cables, in: IEEE Int. Conf. on Intelligent Robots and Systems (IROS), Daejeon, October, 9-14, 2016.

[25] A. Pott, P. Tempel, A unified approach to forward kinematics for cable-driven parallel robots based on energy, in: ARK, Bologna, July, 1-5, 2018.

[26] J.-P. Merlet, The kinematics of cable-driven parallel robots with sagging cables: preliminary results, in: IEEE Int. Conf. on Robotics and Automation, Seattle, May, 26-30, 2015, pp. 1593–1598.

[27] J.-P. Merlet, On the inverse kinematics of cable-driven parallel robots with up to 6 sagging cables, in: IEEE Int. Conf. on Intelligent Robots and Systems (IROS), Hamburg, Germany, September 28- October 2, 2015, pp. 4536–4361.

[28] J.-P. Merlet, Some properties of the Irvine cable model and their use for the kinematic analysis of cable-driven parallel robots, in: EUCOMES, Aachen, September, 4-6, 2018.

[29] E. Hansen, Global optimization using interval analysis, Marcel Dekker, 2004.

[30] L. Jaulin, M. Kieffer, O. Didrit, E. Walter, Applied Interval Analysis, Springer-Verlag, 2001.

[31] J.-P. Merlet, ALIAS: an interval analysis based library for solving and analyzing system of equations, in: SEA, Toulouse, June, 14-16, 2000.

[32] A. Neumaier, Interval methods for systems of equations, Cambridge University Press, 1990.

[33] P. Ciarlet, J.-L. Lions, Handbook of numerical analysis, 7 : solution of equations in Rn (part 3), North-Holland, 2000.

[34] J.-P. Merlet, Determination of the minimal and maximal real roots of parametric polynomials using interval analysis, in: 1st Int. Workshop on Global Constrained Optimization and Constraint Satisfaction (Cocos'02), Valbonne, October, 2-4, 2002, published in LNCS Volume 2861 / 2003,pp. 71-86.

[35] R. Tapia, The Kantorovitch theorem for Newton's method, American Mathematic Monthly 78 (1.ea) (1971) 389–392.